AIP | Applied Physics Letters

Effect of the short collection length in silicon microscale wire solar cells

Hyunyub Kim, Joondong Kim, Eunsongyi Lee, Dong-Wook Kim, Ju-Hyung Yun, and Junsin Yi

Citation: Applied Physics Letters **102**, 193904 (2013); doi: 10.1063/1.4804581
View online: http://dx.doi.org/10.1063/1.4804581
View Table of Contents: http://scitation.aip.org/content/aip/journal/apl/102/19?ver=pdfcov
Published by the AIP Publishing

Effect of the short collection length in silicon microscale wire solar cells

Hyunyub Kim,[1] Joondong Kim,[2,a)] Eunsongyi Lee,[3] Dong-Wook Kim,[3] Ju-Hyung Yun,[4] and Junsin Yi[1]
[1]*School of Information and Communication Engineering, Sungkyunkwan University, Suwon 440746, South Korea*
[2]*Department of Electrical Engineering, Kunsan National University, Kunsan 753701, South Korea*
[3]*Department of Physics, Ewha Womans University, Seoul 120750, South Korea*
[4]*Department of Electrical Engineering, State University of New York, University at Buffalo, Buffalo, New York 14260, USA*

(Received 16 February 2013; accepted 24 April 2013; published online 13 May 2013)

Electrical and optical properties of silicon microscale wire (SiMW) solar cells were investigated. Diverse designs were applied for SiMW geometries as light absorbers. Finite-difference time-domain simulation shows a focused optical field in the wires inducing an optical absorption enhancement in SiMW solar cells. SiMW solar cells provided remarkably higher V_{oc} values (0.597-0.61 V) than that of the planar solar cell (0.587 V). As for the electrical aspects, the position of the space charge region in a SiMW directly affects the carrier collection efficiency according to the SiMW diameter and significantly modulates the photogenerated-currents and voltages in solar cells. © *2013 AIP Publishing LLC*. [http://dx.doi.org/10.1063/1.4804581]

Si is a dominant solar material; it has a low toxicity and is the second most abundant element in the earth, giving the opportunity for its use in low-cost photovoltaics for large-scale deployment.[1,2] However, the inherent limit of Si is that it has an indirect band gap of 1.1 eV resulting in limited optical absorption.[3]

In terms of the optical aspect, an efficient front surface design, where the incident light comes in, is crucially important to the performance of photon absorption.[1,4,5] Lambertian light trapping can be attained when the light active surface is ideally rough to extend the optical path length with a reduced material quantity.[6–8] Various approaches have been applied to improve the incident light utilization in a Si absorber using textured structures, periodic gratings, photonic crystals, and nanostructure-arrays.[6,9–11]

Another important issue is that the electrical design be performed to allow for an effective collecting scheme for photogenerated carriers. Otherwise, the photogenerated carriers will fade away by recombination, resulting in the loss of photovoltaic effects.[8–12] This is a typical reason for the degraded efficiency[13–19] of artificially patterned Si solar cells compared to that of conventional textured Si.[20] Surface enlargement is an identical advantage of nanostructures bearing the potential for improved solar cell performance; however, this simultaneously increases the surface recombination process, hindering the improved performance of the patterned light absorbers.[20] And thus, the effect of defect tolerance cannot be realized in wire-arrayed solar cells.[7]

A productive solar cell should efficiently convert the optical benefit obtained from the light absorber to electric power generation with little electrical loss.[20] Although a number of studies have focused on optical management, little attention has been given to efficient collection scheme for photogenerated carriers in patterned light-absorbing structures. An efficient solar cell should simultaneously considered both the optical and the electrical aspects.[1,20] For optical benefit, a large optical path length is urgently required to keep the incident light for a longer period of time in the light absorber.[7,21] However, a short collection length is absolutely necessary for the effective collection of photogenerated-carriers, in order to minimize the electrical loss caused by recombination.[12]

We herein present an effective design scheme of positioning a space charge region (SCR) in microscale patterned Si wire solar cells. A strong electric field exists in SCR and which provides a higher probability of photogenerated carriers than do other regions in the light-absorber. The spatial distribution of the SCR directly controls the collection length of the photogenerated-carriers in SiMW solar cells.

Four-different microscale SiMW structures were simultaneously fabricated on a 4 in., Chokralsky grown 500 μm-thick, p-type (100) Si wafer having a resistivity of 1-10 Ω cm. Photoresist (PR) patterns were formed on a Si substrate, which worked as protective masks during the reactive ion etching. By removing the PR masks, periodic SiMW structures were achieved on a single wafer with identical depths of 2 μm.

For p-n junction formation, n-type doping was performed both for a pillar structured Si wafer and for a flat Si wafer. Phosphorous oxychloride ($POCl_3$) as an n-type doping source was driven into a furnace for 40 min at 800 °C. A buffered hydrofluoric acid (5% HF) solution was used to remove phosphosilicate glass (PSG). After that, a thin SiN_x layer was deposited by plasma-enhanced chemical vapor deposition (PECVD, SNTEK). The SiN_x-film passivates the n-type doped emitter Si layer and also works as an anti-reflection coating. All samples were tailored to a size $3.2 \times 3.2\,cm^2$. For the front and the rear metal contacts, Ag paste and Al paste were screen-printed in advance for each device; after this, a co-firing process was applied.

A field emission scanning electron microscope (FESEM, FEI Sirion) was used to observe the Si structures. Four-different Si absorbers (Fig. 1(a)) were simultaneously

a)Author to whom correspondence should be addressed. Electronic mail: joonkim@kunsan.ac.kr. Tel.: +82-63-469-4741. Fax: +82-63-469-4699.

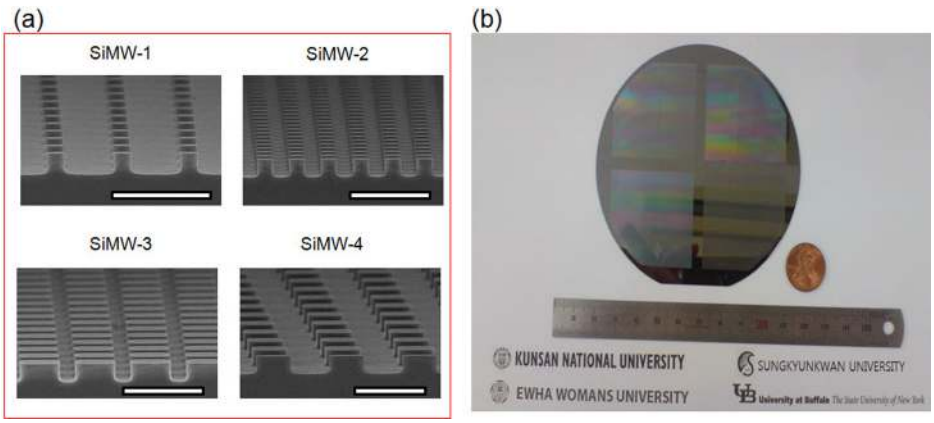

FIG. 1. Microscale patterned Si wafer. (a) Four-different Si absorbers were designed having different diameters and periods at fixed depth, scale bars represent 10 μm. (b) A photograph of a 4 inch Si wafer having SiMW patterns on four quadrants.

TABLE I. Geometric information and solar cell performances.

Sample	Diameter [μm]	Period [μm]	Efficiency [%]	V_{oc} [V]	J_{sc} [mA/cm^2]
SiMW-1	2	7	15.8	0.599	35.0
SiMW-2	2	4	16.2	0.610	35.44
SiMW-3	5	7	15.8	0.597	35.4
SiMW-4	5	10	15.0	0.591	34.65
Planar Si	N/A	N/A	14.3	0.587	33.9

fabricated on an identical Si wafer as shown in Fig. 1(b). Each SiMW structure had a different diameter and a period at a fixed depth of about 2 μm. One geometric couple can be made with SiMW-1 and SiMW-2. SiMW-1 has a diameter of 2 μm with a 7 μm period. SiMW-2 has a similar diameter of 2 μm with a smaller period of 4 μm. The other couple is paired by SiMW-3 and SiMW-4, which have similar diameters of 5 μm. However, there are different periods of 7 μm for SiMW-3 and 10 μm for SiMW-4. These structural changes are factors that modulate the spectral responses of

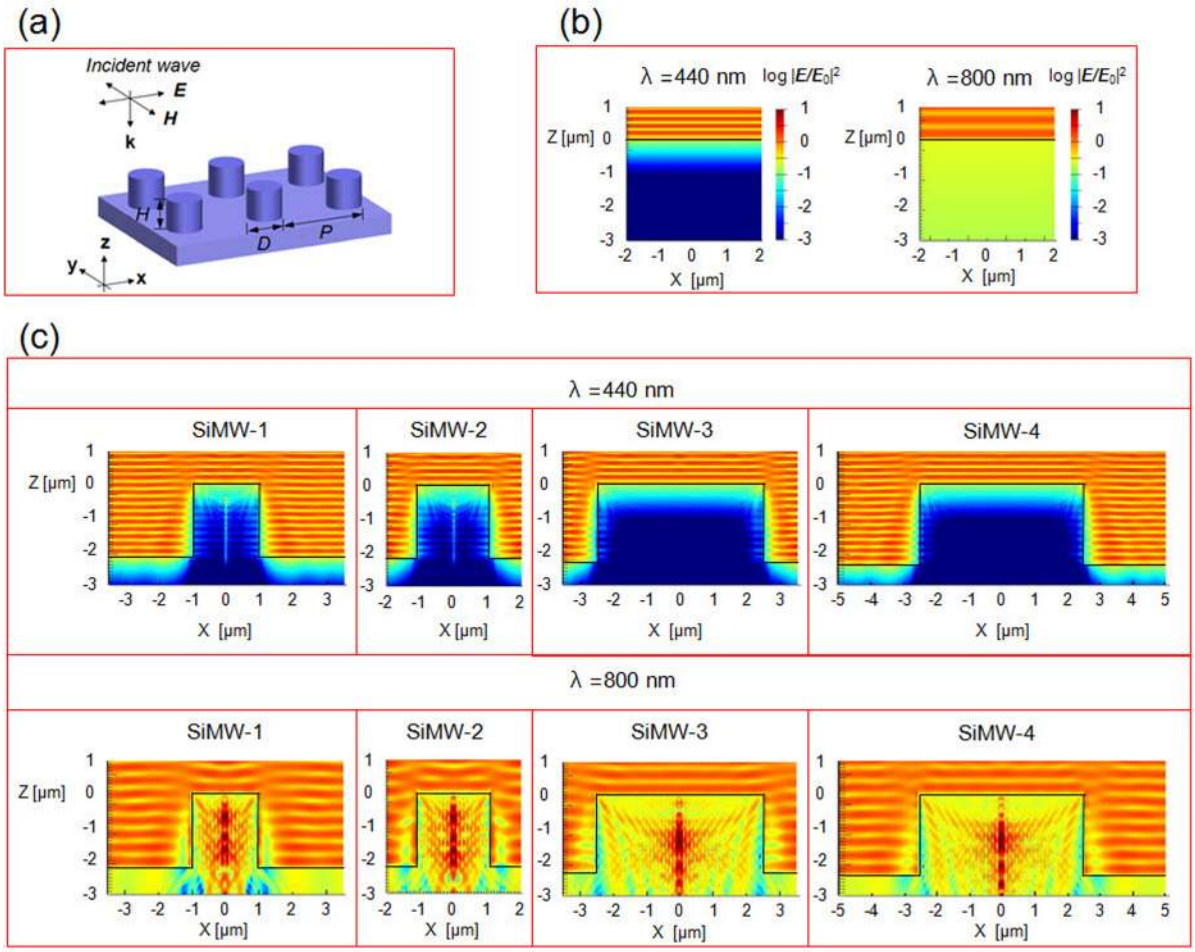

FIG. 2. FDTD simulation. (a) Schematic of modeling; Optical electric field distribution profiles through (b) a planar Si absorber and (c) SiMW absorbers.

Si solar cells.[6,9,22,23] The geometric information of SiMW structures and solar cell performances are shown in Table I.

Real-space optical field distributions in SiMWs and in planar Si were investigated using finite-difference time-domain (FDTD) method (Lumerical FDTD Solutions). A broad-band pulse (wavelength 400-1100 nm) was used to simulate a plane wave incident from the top; the polarization and propagation directions of this wave were parallel to the x-axis and the z-axis, respectively, as shown in Fig. 2(a), in which P, D, and H stand for period, pillar diameter, and height, respectively.

For a short wavelength (λ) of 440 nm, the incident light exponentially decays from the surface due to the high absorption coefficient of Si for short wavelengths as shown in Fig. 2(b) for planar Si. This means that the incident light is only effective at a thin depth of the Si absorber, resulting in slight differences of incident light profile in SiMW structures (see Fig. 2(c)). However, a significantly different profile was observed for a long wavelength of 800 nm. The pillar structures drove guided-mode-excitation through the Si body and formed a peak field distribution in the center of a pillar. In addition, a smaller SiMW diameter of 2 μm (SiMW-1 or SiMW-2) has a more intensive field distribution between the SiMW center and the boundary than does a larger pillar with a diameter of 5 μm (SiMW-3 or SiMW-4).

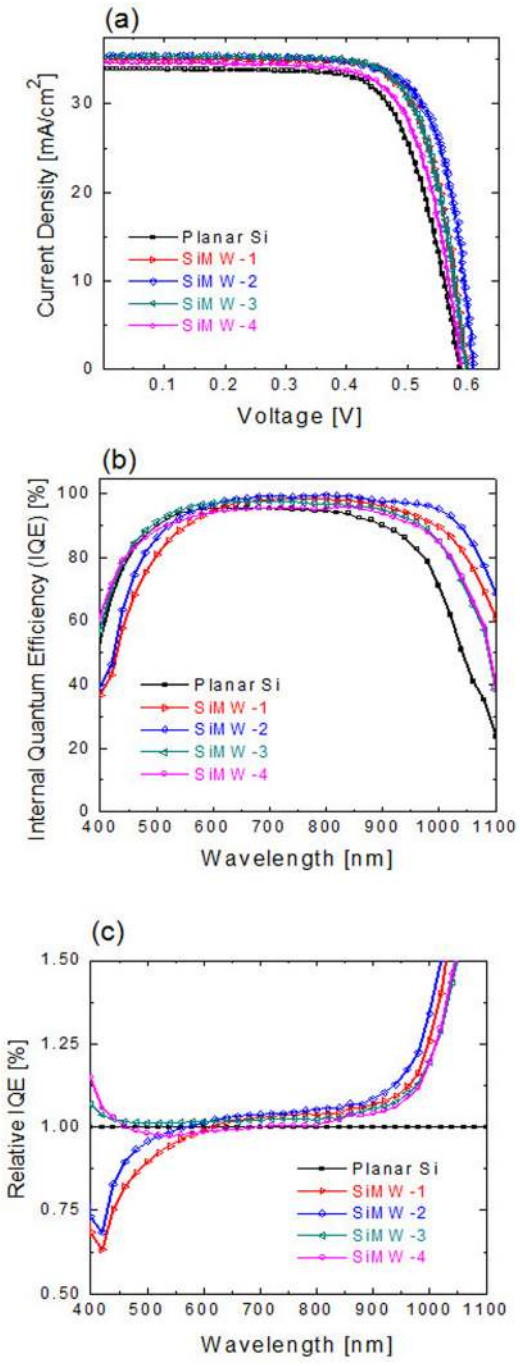

FIG. 3. Solar cell performances (a) under one sun illumination. (b) IQE profiles. (c) Relative IQE values of SiMWs compared to that of a planar Si.

Under one-sun illumination (AM 1.5, 100 mW/cm^2), SiMW-2 provided the highest short-circuit current density (J_{sc}) among the patterned SiMW absorbers as shown in Fig. 3(a), corresponding to the design rule of maximum current when hole depth is equal to half of a period.[22,23] SiMW-2 exhibited a J_{sc} of 35.44 mA/cm^2 and an open-circuit voltage (V_{oc}) of 0.610 V, giving a conversion efficiency (η) of 16.2%. These results indicate significantly improved performance compared to that of the reference cell, which showed an efficiency of 14.3% with J_{sc} of 33.9 mA/cm^2 and V_{oc} of 0.587 V.

It is interesting to observe the effect of SiMW diameter. Smaller diameter (2 μm) SiMW arrays (SiMW-1 and SiMW-2) showed a stronger field intensity inside a SiMW geometry than the field intensity of larger diameter (5 μm) SiMW arrays (SiMW-3 and SiMW-4). This clearly improved the J_{sc} in SiMW-2 solar cell compared to that of SiMW-3 or SiMW-4 solar cell. However, SiMW-1 has a lower J_{sc} (35 mA/cm^2) than that of SiMW-3 (35.4 mA/cm^2) due to the sparse distribution of wire-arrays along the period.

For further investigation, we performed internal quantum efficiencies (IQEs) for SiMW solar cells and for a planar (reference) device, as shown in Figs. 3(b) and 3(c). The collection probability of photogenerated carriers is a function of the effective utilization of the incident light inside a light-absorber, which directly affects the photogenerated current.

The red light region (around 650 nm) is the most important wavelength for a Si absorber.[8] At the corresponding wavelength, the IQE of SiMW-2 was measured and found to be 98.67% as shown in Fig. 3(b). This is a higher value than that of 95.72% for a flat Si, which is a distinctive result for a nanostructured Si absorber,[20] indicating a relieved burden of recombination loss in the microscale Si absorber.

The relative IQE values of Fig. 3(c) clearly represent the collection efficiencies of SiMW solar cells comparing to that of a planar device. For long wavelengths (above 700 nm), a clearly improved IQE value was obtained from all SiMW devices compared to that of the planar cell (Fig. 3(c)). At a wavelength of 1100 nm, a substantial IQE enhancement of 289% was obtained using the SiMW-2 device from the reference cell as shown in Fig. 3(c).

At a short wavelength at 400 nm, however, a reduction of the IQE value was obtained from the smaller SiMW diameter (2 μm) solar cells. SiMW-1 has only 68.5% and SiMW-2 has 73% of the IQE value of the reference. For comparison, SiMWs having a larger diameter (5 μm) showed enhanced IQE values of 107% (SiMW-3) and 115% (SiMW-4). These results strongly show the co-existence of the optical benefit and the electrical concern according to the surface enhancement in a light absorber. The array structures easily provide a high cross-sectional surface; this surface definitely

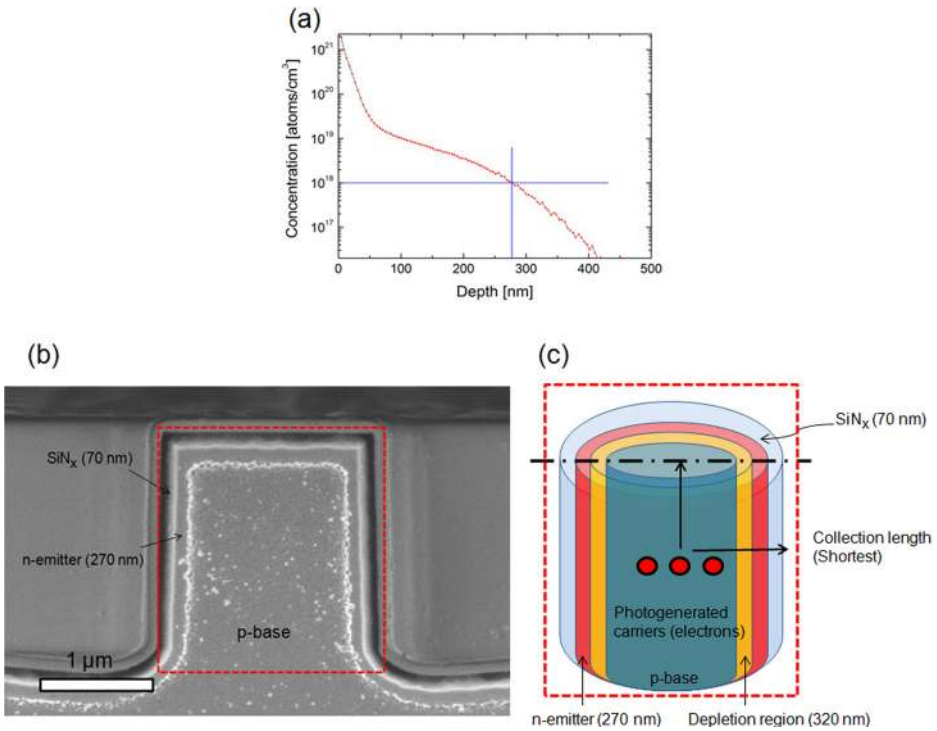

FIG. 4. Junction profiles. (a) SIMS profile of n-doping concentration. (b) a LVSEM image showing n-p junction with a SiN_x coating layer. (c) Schematic of junction formation inside a SiMW absorber. Note that the schematic is not drawn to scale.

contributes to the optical enhancement. However, the patterning process almost always accompanies with surface defects, causing a recombination problem[13,20] that deteriorates the photogenerated-carrier collection. This is considered a controversial issue in realizing good defect tolerance for wire arrays.[7] In our results, 5 μm-diameter SiMWs show that the optical benefit surpasses the surface recombined electrical loss, resulting in an increased IQE. However, at short wavelengths, the surface recombination dominates the overall IQE performance for 2 μm-diameter SiMWs, nullifying the optical enhancement according to the reduction of carrier collection efficiency. The surface recombination phenomenon is prominent for short wavelengths since the incident light decays at the thin depth of the Si absorbers (Fig. 2), where there is a heavily n-doped Si emitter region.

To determine the emitter depth from the SIMS profile, the n-doping concentration value was found at a point of doping density (10^{18}/cm^3) 100 times higher than that of the p-doped Si base (10^{16}/cm^3) as shown in Fig. 4. According to this, the emitter depth was obtained to be 270 nm. When the carrier concentration is greater than 10^{17}/cm^3 (Ref. 24) or 10^{18}/cm^3 (Ref. 20), Auger recombination also affects the collection efficiency.

We have performed low-voltage SEM (LVSEM) analysis to investigate the regional junction in the SiMW structure. An LVSEM image enables us to clarify the junction formation inside the SiMW as shown in Fig. 4(b). A heavily doped n-type emitter layer was clearly observed, adjacent to a p-type Si base. A 70 nm SiN_x film is sitting on a Si absorber.

Considering an ideal p-n junction, a space charge region (also called a depletion region) is formed, resulting in the freeing of majority carriers. The total depletion width (W) is the sum of W_p into the p-side and W_n into the n-side. Due to the doping concentration of the n-side (10^{18}/cm^3), which is two orders of magnitude higher than that of the p-side (10^{16}/cm^3), the most space charge region (99%) deploys into the p-base Si base as presented in Fig. 4(c). The depletion width in the p-n junction can be obtained according to the following equation:

$$W = (2\varepsilon_0\varepsilon_r V_b/qN_a)^{1/2}, \quad (1)$$

where ε_0, ε_r, V_b, q, and N_a are the permittivity of vacuum, dielectric constant, built-in potential, quantity of electric charge, and acceptor doping density, respectively.

The built-in potential (V_b) can be calculated by

$$V_b = (kT/e)\ln(N_aN_d/n_i^2), \quad (2)$$

where k, T, e, N_a, N_d, and n_i are the Boltzman constant, electron charge, temperature, acceptor doping density, donor doping density, and the intrinsic carrier density, respectively. By calculation, we extracted a value of V_b of 0.816 V, and thus the depletion width is obtained and found to be 328 nm.

The reference values of J_{sc} (33.9 mA/cm^2) and V_{oc} (0.587 V) are very close to the values determined using the modeling calculations.[12] This strongly suggests that the depletion region was formed inside the n-emitter/p-base junction, indicating a little concern about the recombination in SCR. This enables us to ignore the problem of the density of recombination centers in the quasi-neutral region.[12]

All core/shell structured SiMW solar cells provided improved J_{sc} values (35-35.44 mA/cm^2); these values are comparable to those determined using the modeling calculations.[12] Although the J_{sc} improvements were achieved using SiMW absorbers, the surface-defects induced recombination loss and diminished the J_{sc} boosting effect of the core/shell SiMW solar cells, especially for short wavelengths, as previously stated in the IQE profiles.

Despite the only slightly increased J_{sc} values, our SiMW solar cells provided remarkably higher V_{oc} values

(0.597-0.61 V) than that of the planar solar cell (0.587 V); these are distinctive results for the modeling expectations.[12] The variation of V_{oc} strongly depends on the trap density in an SCR. When the depletion region is fairly well formed, the value of V_{oc} is relatively high, regardless of the quality of the quasi-neutral region. For radial n/p structures, the value of V_{oc} typically tends to decrease as the junction area increases due to the recombination problem in the depletion region.[12]

A distinctive result is obtained in our radial n-emitter shell/p-base core SiMW solar cells. The substantially enhanced value of V_{oc}, which is due to the SiMW structure, can be explained by the position of an SCR in the Si absorbers. Each SiMW has a different diameter, giving variations in the distance between the SCR and the center of the SiMW; this circumstance is directly related to the carrier collection length. From the FDTD simulation, the peak waveguide mode is generated in the center of the SiMWs. This suggests that the most photogenerated carriers are initially produced along the center position. Due to the different diameters of the SiMWs, each SiMW solar cell has a different collection length of the photogenerated minority carriers.

In summary, the SiMW structure is effective to produce a focused electric field in a wire center. A smaller diameter (2 μm) SiMW has a stronger electric field between the boundary and the wire center than does a larger diameter (5 μm) SiMW, resulting in an improved solar cell performance.

All SiMWs substantially increased the IQE values of a planar substrate for long wavelengths. A smaller diameter SiMW has a shorter collection length for photogenerated carriers resulting in improved overall conversion efficiencies.

A SCR has a higher collection probability than that of other regions in a Si absorber. As for electrical aspects, the position of the SCR in a SiMW directly affects the collection length according to the diameter and significantly modulates the photogenerated-currents and voltages. This strongly suggests an effective design of radial n/p structured Si solar cells both for electrical and optical aspects.

The authors acknowledge the financial support of the Korea Institute of Energy Technology Evaluation and Planning grant funded by the Ministry of Knowledge and Economy (KETEP-20113030010110) and the Converging Research Center Program through the Ministry of Education, Science and Technology (MEST, 2012K001278).

[1]M. G. Deceglie, V. E. Ferry, A. P. Alivisatos, and H. A. Atwater, Nano Lett. **12**, 2894 (2012).
[2]Y. Liu, T. Lai, H. Li, Y. Wang, Z. Mei, H. Liang, Z. Li, F. Zhang, W. Wang, A. Y. Kuznetsov, and X. Du, Small **8**, 1392 (2012).
[3]L. Hu and G. Chen, Nano Lett. **7**, 3249 (2007).
[4]J. Kim, M. Kim, H. Kim, K. Song, E. Lee, D.-W. Kim, J.-H. Yun, B.-I. Choi, S. Lee, C. Jeong, and J. Yi, Appl. Phys. Lett. **101**, 143904 (2012).
[5]S.-W. Jee, S.-J. Park, J. Kim, Y. C. Park, J.-H. Choi, J.-H. Jeong, and J.-H. Lee, Appl. Phys. Lett. **99**, 053118 (2011).
[6]S. E. Han and G. Chen, Nano Lett. **10**, 4692 (2010).
[7]H. Alaeian, A. C. Atre, and J. A. Dionne, J. Opt. **14**, 024006 (2012).
[8]S. E. Han and G. Chen, Nano Lett. **10**, 1012 (2010).
[9]Q. G. Du, C. H. Kam, H. V. Demir, H. Y. Yu, and X. W. Sun, Opt. Lett. **36**, 1713 (2011).
[10]L. He, D. Lai, H. Wang, C. Jiang, and Rusli, Small **8**, 1664 (2012).
[11]Y. Li, H. Y. Yu, J. Li, S.-M. Wong, X. W. Sun, X. Li, C. Cheng, H. J. Fan, J. Wang, N. Singh, P. G.-Q. Lo, and D.-L. Kwong, Small **7**, 3138 (2011).
[12]B. M. Kayes, H. A. Atwatera, and N. S. Lewis, J. Appl. Phys. **97**, 114302 (2005).
[13]D. R. Kim, C. H. Lee, P. M. Rao, I. S. Cho, and X. Zheng, Nano Lett. **11**, 2704 (2011).
[14]K.-Q. Peng, X. Wang, X.-L. Wu, and S.-T. Lee, J. Am. Chem. Soc. **132**, 6872 (2010).
[15]Y. Lu and A. Lal, Nano Lett. **10**, 4651 (2010).
[16]K.-Q. Peng and S.-T. Lee, Adv. Mater. **23**, 198 (2011).
[17]M. D. Kelzenberg, S. W. Boettcher, J. A. Petykiewicz, D. B. Turner-Evans, M. C. Putnam, E. L. Warren, J. M. Spurgeon, R. M. Briggs, N. S. Lewis, and H. A. Atwater, Nat. Mater. **9**, 239 (2010).
[18]J.-Y. Jung, Z. Guo, S.-W. Jee, H.-D. Um, K.-T. Park, M. S. Hyun, J. M. Yang, and J.-H. Lee, Nanotechnology **21**, 445303 (2010).
[19]E. Lee, Y. Kim, M. Gwon, D.-W. Kim, S.-H. Baek, and J. H. Kim, Sol. Energy Mater. Sol. Cells **103**, 93 (2012).
[20]J. Oh, H.-C. Yuan, and H. M. Branz, Nat. Nanotechnol. **7**, 743 (2012).
[21]X. Meng, E. Drouard, G. Gomard, R. Peretti, A. Fave, and C. Seassal, Opt. Express **20**, A560 (2012).
[22]R. Dewan and D. Knipp, J. Appl. Phys. **106**, 074901 (2009).
[23]C. Lin and M. L. Povinelli, Opt. Express **17**, 19371 (2009).
[24]X. X. Liu and J. R. Sites, J. Appl. Phys. **75**, 577–581 (1994).